Poly(*n*-butyl acrylate-*co*-carbon monoxide-*co*-ethylene) Characterization by High-Temperature Two-Dimensional NMR at 750 MHz

Faith J. Wyzgoski and Peter L. Rinaldi*

Department of Chemistry, The University of Akron, Akron, Ohio 44325-3601

Elizabeth F. McCord, Mark A. Stewart, and Donald R. Marshall

E. I. du Pont de Nemours and Co., Inc., Wilmington, Delaware 19880-0101

Received September 4, 2003; Revised Manuscript Received October 15, 2003

ABSTRACT: Poly(*n*-butyl acrylate-*co*-carbon monoxide-*co*-ethylene) samples with varying monomer compositions and degrees of branching (g') were characterized using 750 MHz two-dimensional (2D) pulsed-field gradient (PFG) NMR spectroscopy. The NMR experiments were performed in solution at 100 °C to ensure sample homogeneity and sufficient mobility of the ethylene-based terpolymer. Since the ^{1}H and ^{13}C NMR spectra of the terpolymer samples were complex, 2D-^{1}H/^{13}C-heteronuclear multiple quantum coherence (HMQC) and heteronuclear multiple bond correlation (HMBC) experiments were conducted. The distinctive resonances of the ketone and ester carbonyl groups facilitated spectral assignments, such that chain-end resonances were apparent and the effects of short-chain-branching reactions and monomer sequence distributions were readily observed.

Introduction

Copolymers of polyethylene are used in a variety of applications and are frequently employed as additives that affect such properties as melting points, tensile strength, and flexibility. Ethylene/acrylate/carbon monoxide terpolymers are often utilized as modifying agents for poly(vinyl chloride), polyester, and poly(acrylonitrile-*co*-butadiene-*co*-styrene). Understanding the structure of these ethylene-based terpolymers permits design of materials with specific physical properties. Nuclear magnetic resonance (NMR) experiments contribute valuable structural data to explain how variation of process conditions influences terpolymer structure and properties.

Recently, high-temperature one- and two-dimensional nuclear magnetic resonance (NMR) experiments have yielded unambiguous structural information for samples of polyethylene and ethylene/1-alkene copolymers.[1,2] Employing pulsed-field gradients (PFG) with 2D-NMR at high field (750 MHz) permitted resolution of ^{13}C resonances from minor structural components; unique ^{13}C spectral assignments were reported in branches up to 10 carbons long.[3] These NMR techniques have just recently been applied to a series of ethylene/1-octene[4] and ethylene/1-butene copolymers[5] affording assignments of new ^{13}C resonances and confirmation of assignments previously made by empirical means. Herein is reported that similar NMR methods can be employed to assign the resonances of terpolymer samples of poly(*n*-butyl acrylate-*co*-carbon monoxide-*co*-ethylene), polyBCE, for use in structure/property relationship studies. This work details results from high-temperature (100 °C) 1D and 2D PFG heteronuclear multiple quantum coherence (HMQC)[6,7] and heteronuclear multiple bond correlation (HMBC)[8] experiments at 750 MHz.

Most NMR work to date has involved the study of homo- and copolymers. Because of their complexity, very little work has been published on the thorough NMR characterization of terpolymers. Previous research at lower field strengths has yielded resonance assignments for copolymers such as poly(ethylene-*co*-carbon monoxide) using 1D[9,10] and 2D[11] NMR methods. NMR characterizations of ethylene-based terpolymers such as poly(carbon monoxide-*co*-ethylene-*co*-ethyl acrylate)[12] and poly(carbon monoxide-*co*-ethylene-*co*-methyl acrylate)[11] have also been reported. In addition, McCord et al.[13] analyzed ethylene copolymers of various compositions including poly(*n*-butyl acrylate-*co*-ethylene) using ^{1}H, ^{13}C, and 2D NMR techniques. They reported the presence of short-chain-branching (SCB) structures in these polymers obtained by free-radical-initiated polymerization. These SCB structures (length 5 or shorter) were a result of both hydrogen abstraction from polyethylene CH_2 units and H abstraction from comonomer units. SCB was postulated as an important occurrence in these ethylene/acrylate copolymers affecting the polymers' physical properties. NMR results described in this paper demonstrate a relationship between SCB and the comonomer content of the polyBCE terpolymer samples.

Experimental Section

Preparation of Polymers. Three samples labeled as A, B, and C of polyBCE were prepared using free radical polymerization at E. I. du Pont de Nemours and Co. Carbon monoxide was obtained from Messer/MG, *n*-butyl acrylate from Celanese, and ethylene from Sun. Initiation occurred via thermal decomposition of organic peroxides. Samples were produced with a flow-through stirred autoclave pilot-plant reactor using high temperature (150−300 °C) and pressure (15−40 kpsi) reaction conditions. The polymer samples were degassed in a polymer separator, fed to a melt pump, and strand cut when feasible. The monomer compositions (mol %, determined by 1D ^{13}C NMR) and characteristics of these samples are summarized in Table 1.

Gel Permation Chromatography. Number- and weight-average molecular weights and g' values (Table 1) were obtained at E. I. du Pont de Nemours and Co. with GPC columns (20 m) designed for high molecular weight polymer

* Corresponding author: Tel 330-972-5990; Fax 330-972-5256; e-mail PeterRinaldi@uakron.edu.

10.1021/ma035311j CCC: $27.50
Published on Web 01/09/2004

Table 1. Physical Properties of Poly(*n*-butyl acrylate-*co*-carbon monoxide-*co*-ethylene) Samples

sample	A	B	C
composition, mol % B/C/E	10/12/78	14/13/73	8/26/66
M_n (g mol^{-1})	13931	14167	11316
M_w (g mol^{-1})	519472	506576	594800
M_w/M_n	37.3	35.8	52.6
M_I	6.9	8.0	65.0
g'(av)	0.329	0.325	0.151

separations. Data reduction was done using Waters Millennium 32 GPCV software that fits intrinsic viscosity and molecular weight data to the classic Zimm−Stockmayer equation.[14] The output from this fit is a measure of the Mark−Houwink relationship for the linear polymer and the value of g', the ratio of intrinsic viscosities, branched to linear across the distribution.

Melt Index. The melt index, M_I, of the terpolymer samples was obtained by a test method following ASTM D 1238-01 Procedure A (190 °C/2.160 kg).[15] Molten resins were extruded through a die meeting ASTM specifications. Conditions (temperature/weight) were selected so that the molten polymer flow rate fell between 0.15 and 50 g/10 min. Measurements made at conditions other than that for melt index were converted to approximate flow at 2160 g and 190 °C for comparison.

Preparation of Terpolymer Samples for NMR Analysis. The NMR samples were 10% w/v solutions of polymer in a solvent composed of benzene-d_6 (20% w/v) and 1,2,4-trichlorobenzene; a trace of hexamethyldisiloxane was added as internal standard ($\delta_C = 2.0$ ppm). To obtain a homogeneous solution, the solid sample was placed in the NMR tube, and enough solvent was added to cover the material. The sample tube was secured to the rotating arm of a Kugelrohr apparatus via Tygon tubing and horizontally positioned in the Kugelrohr's hot air oven at 100 °C. The tube was slowly rotated until the solid dissolved; 0.5 mL of solvent was added to the tube and rotation resumed. Incremental additions of solvent followed by rotation continued until a homogeneous solution was observed. The sample tube was rotated for at least an additional 30 min. The tube was then removed from the apparatus, closed with a Teflon cap, and transferred to the NMR probe. The sample was allowed to equilibrate in the probe for approximately 1 h before acquiring spectra.

Acquisition of 1D ^{13}C NMR Spectra. The 1D ^{13}C NMR spectra were obtained on a Varian UNITYplus 750 MHz spectrometer with a 10 mm broadband (^{15}N−^{31}P) probe at 100 °C, with a 8.1 μs (60 °) pulse, 128 kHz spectral width, 1.5 s acquisition time, and 30 s relaxation delay. The spectra were obtained with continuous WALTZ-16 modulated decoupling. The data were zero-filled to 512k and exponentially weighted with a 1 Hz line broadening before Fourier transformation. Quantitative ^{13}C NMR results were obtained in a similar manner, except a 12.1 μs (90°) pulse and gated WALTZ-16 modulated decoupling were used. Three separate spectra of the same sample were collected and added.

^{13}C distortionless enhancement by polarization transfer (DEPT)[16] experiments were performed on all three samples at 100 °C to determine the multiplicity of ^{13}C resonances. DEPT spectra were acquired with a Varian UNITYplus 750 MHz spectrometer with a 5 mm broadband (^{15}N−^{31}P) probe. The spectra were obtained with 90° pulse widths for ^{13}C and ^{1}H of 8.0 and 19.0 μs, respectively, a relaxation delay of 6 s, 1.8 ms polarization transfer delays (based on $^1J_{CH} = 140$ Hz), a 25 kHz spectral width, and a 2.5 s acquisition time (with WALTZ-16 decoupling).

Acquisition of PFG-HMQC and HMBC 2D NMR Spectra. The 2D HMQC NMR spectra were collected on a Varian UNITYplus 750 MHz spectrometer with a Nalorac ^{1}H/^{2}H/^{13}C/X (X tunable between the frequencies of ^{2}H and ^{31}P) 5 mm pulsed field gradient (PFG) probe designed to operate up to 130 °C. The spectra were obtained with 90° pulse widths for ^{1}H and ^{13}C of 11.3 and 37.0 μs, respectively, a 2 s relaxation delay, $\Delta = 1.8$ ms (based on $^1J_{CH} = 140$ Hz), and a 0.048 s acquisition time (with ^{13}C GARP[17] decoupling). Thirty-two transients were averaged for each of 512 increments during t_1. The evolution time was incremented to provide the equivalent of a 14.2 kHz spectral width in the f_1 dimension, and a 6.0 kHz spectral width was used in the f_2 dimension. The PFG pulses were 2.0 ms in duration and had amplitudes of 0.2000 and 0.149 60 T/m for the first and second PFG pulses. The experiment time was ca. 9 h. Data were zero-filled to a 2048 × 4096 matrix and weighted with a sinebell function before Fourier transformation.

HMBC spectra were obtained in a similar manner, except that the acquisition time was 0.341 s and two separate spectra were collected with f_1 spectral windows of 10 kHz (ketone and ester carbonyl region) and 14 kHz (aliphatic carbon region). A 6.0 kHz spectral width was used in the f_2 dimension for both of the spectra. A fixed delay of 0.080 s allowed the long-range heteronuclear antiphase magnetization to evolve for multiple-bond correlations.

Table 2. Possible Triad Sequences for Poly(*n*-butyl acrylate-*co*-carbon monoxide-*co*-ethylene)[a]

EEE	BBB(3)	~~CCC~~
EEB	EBB(2)	~~ECC~~
BEB(2)	EBE	ECE
CEE	CBB(2)/~~BBC~~(2)	~~BCC/CCB~~
CEC	~~CBC~~	~~BCB~~(2)
BEC/CEB	~~EBC~~/CBE	ECB/~~BCE~~

[a] B = *n*-butyl acrylate, C = carbon monoxide, and E = ethylene. The numbers in parentheses indicate the number of triad stereosequences when more than one is possible.

Results and Discussion

Structures and Nomenclature. Interpreting the complex 1D-NMR spectra in this terpolymer study is challenging, even at the triad level. Because of the lack of a methylene group in C≡O, the order of addition is important in determining the monomer-sequence-derived structures (e.g., diad CB is not equivalent to diad BC when included in a sequence of ethylene units as it would be if B and C were both vinyl monomers). If polymerization is assumed to occur solely in a head-to-tail manner, up to 23 unique triad sequences are theoretically possible. If stereosequences due to the acrylate monomer units are considered, the number of triads further increases, as shown in Table 2. However, according to previous studies,[12] carbon monoxide has a low probability of addition to the carbon monoxide-derived ketone carbonyl unit at the end of a propagating chain; therefore, sequences containing CC units can be ignored as shown by strikethroughs for selected entries in Table 2. In addition, analogous to findings for poly(carbon monoxide-*co*-ethylene-*co*-ethyl acrylate),[11] it is assumed in most cases that addition of carbon monoxide to the methine of a butyl acrylate chain end is unlikely due to steric constraints and to the absence of the appropriate NMR resonance for a methine adjacent to a ketone carbonyl unit. Thus, units containing BC diads are also eliminated by strikethroughs in Table 2.

Since the spectra from the terpolymer samples contain resonances characteristic of long sequences of ethylene monomer units, the general structure for polyethylene is shown in Scheme 1. The carbons in this structure are labeled on the basis of nomenclature first defined by Carman[18] and modified by Dorman[19] and Randall.[20] Methylene carbons along the backbone are identified by a pair of Greek letters to indicate the distances to the branches in either direction. Carbons

Scheme 1. Structure and Nomenclature for Polyethylene

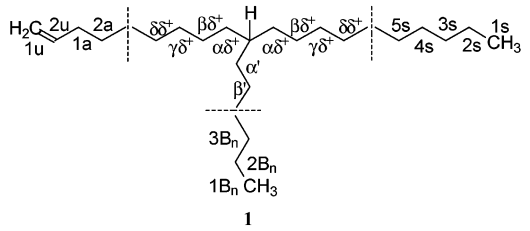

1

Scheme 2. Structures and Nomenclature for Poly(*n*-butyl acrylate-*co*-carbon monoxide-*co*-ethylene)

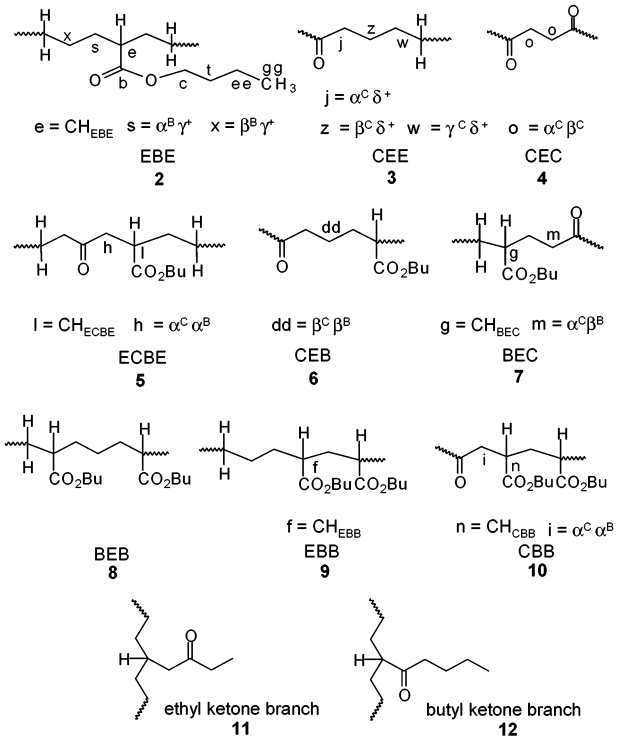

EBE **2** | CEE **3** | CEC **4**

ECBE **5** | CEB **6** | BEC **7**

BEB **8** | EBB **9** | CBB **10**

ethyl ketone branch **11** | butyl ketone branch **12**

in the side chains are designated by iB_n, where "*i*" indicates the position in the branch starting with the methyl in position 1 and the subscript "*n*" denotes the length of the branch.

The terpolymer samples also contain structures resulting from the addition reactions of ethylene and *n*-butyl acrylate. The labeling for the carbons of all butoxy groups and for those carbons in the polymer backbone found in EBE triads is shown by **2** of Scheme 2. A system of nomenclature is proposed to label the backbone carbon atoms occurring in the various structures (Scheme 2) that can be formed during the polymerization process.[21] Methine carbons are labeled according to current convention; e.g., the methine carbon (e) of the EBE triad (**2**) is designated as CH_{EBE}, where the subscript denotes the triad sequence in which the methine is centered. As with ethylene/α-olefin copolymers, a pair of Greek letters is employed to describe the position of each carbon atom relative to a branch. However, the nature of the branch cannot be assumed as is done with ethylene/1-olefin copolymers; it is specified by a superscript B for a butyl acrylate monomer unit and by superscript C for a "branch"[22] formed by the ketone carbonyl. As in the currently used nomenclature for polyethylenes, when the number of methylenes separating a carbon from a branch is greater than a certain number of bonds, a superscripted (+) is

Scheme 3. Possible Short-Chain Branch-Forming Mechanisms Involving Polymerization of Ethylene with *n*-Butyl Acrylate Comonomer[a]

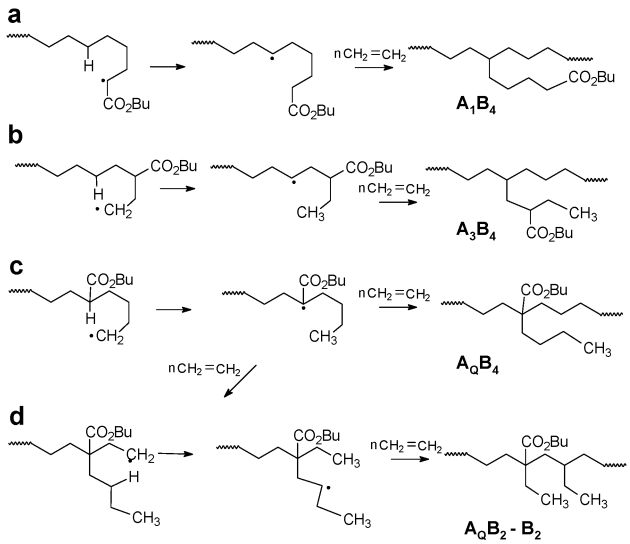

[a] Reactions: (a) H-abstraction by a comonomer radical (formation of A_1B_4 branch); (b) H-abstraction across a comonomer radical (formation of A_3B_4 branch); (c) H-abstraction from a comonomer unit to form A_QB_4 butyl branch (single backbite); (d) double-backbite mechanism involving H-abstraction from a comonomer unit to form $A_QB_2-B_2$ branches.

used. For example, carbon s of the EBE triad (**2**, Scheme 2) is labeled as $\alpha^B\gamma^+$ to indicate this carbon is α to the branch formed by a butyl acrylate monomer unit and that the branch is in the γ position or greater along the polymer backbone in the opposite direction. An example of the nomenclature system for structures resulting from addition reactions of carbon monoxide and ethylene is shown by **3** in Scheme 2, wherein CEE triad methylene carbons j, z, and w are α, β, and γ to a ketone carbonyl group and are designated $\alpha^C\delta^+$, $\beta^C\delta^+$, and $\gamma^C\delta^+$, respectively. The 1,4-dione structure **4** in Scheme 2 contains equivalent methylenes (o) that are designated $\alpha^C\beta^C$ since these carbons are α and β to branches formed from carbon monoxide. Scheme 2 shows other structures with corresponding labels illustrating the nomenclature for describing their carbon atoms.

Additional structures may occur due to short-chain branch-forming reactions involving the *n*-butyl acrylate monomer unit. Scheme 3 illustrates the mechanisms for "backbiting" reactions[23−25] with the nomenclature proposed by McCord et al.[13] for ethylene/acrylate copolymers. An A_1B_4 branch results when *n*-butyl acrylate radical backbites to abstract hydrogen from the δ methylene carbon. The acrylate ester group is found on the end (or "1") carbon of the resulting B_4 branch (Scheme 3a). An A_3B_4 branch occurs when a CH_2 radical backbites around an acrylate unit in the chain (Scheme 3b). It is also possible for a terminal CH_2 radical to abstract hydrogen from a butyl acrylate unit to form a tertiary-centered radical. After chain growth, the resulting alkyl SCB is opposite the *n*-butyl acrylate side chain and forms a quaternary carbon in the polymer backbone that is designated as A_QB_4 (Scheme 3c). Double backbite mechanisms may also occur: Scheme 3d shows a mechanistic pathway to form an A_QB_2 and B_2 sequence.

1D ^{13}C NMR Spectra. The monomer compositions and the physical properties of the three samples of polyBCE are shown in Table 1. The ^{13}C NMR spectra of samples A, B, and C, shown in Figure 1, have

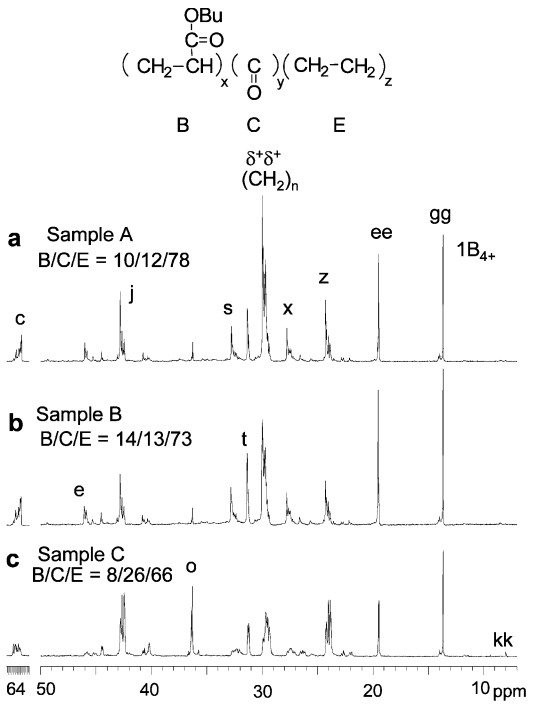

Figure 1. 188 MHz ^{13}C NMR spectra of poly(*n*-butyl acrylate-*co*-carbon monoxide-*co*-ethylene) samples having varied monomer compositions: (a) sample A, (b) sample B, and (c) sample C.

characteristics that reflect their compositions. The spectrum of sample A, with the highest concentration of ethylene monomer units, has the most intense $\delta^+\delta^+$ peak (30.08 ppm). Sample C, with the highest ketone carbonyl level relative to A and B, exhibits the highest concentration of 1,4-dione-type structure 4, as indicated by the high intensity of o-type peaks near δ = 36.35. The spectrum of sample C also has the most intense peaks near 42.91 (j) and 24.31 ppm (z) for methylenes α and β to the ketone carbonyls of CEE triads. As expected, the intensities of peaks j and z are similar in each of the three spectra, since similar numbers of α and β backbone methylenes should be formed upon insertion of C═O into the polymer.

Figure 2 shows expansions of selected regions from the spectra in Figure 1. A comparison of the 7−12 ppm region (Figure 2a) from the ^{13}C NMR spectra of the three samples reveals the effect of increased ketone carbonyl content on the chain-end structures. The spectrum of sample C shows increased intensity for the peak at δ = 8.02, the resonance attributed to the terminal methyl of CE diads at chain ends or on branches terminating in ethyl ketone units (e.g., 11).[11] Decreased intensity is observed for the peak at 8.51 ppm, which is attributed to the methyl in an ethyl branch attached to the same quaternary backbone carbon as the acrylate branch resulting from short chain branching ($1A_QB_2$ of Scheme 3d).[13]

The effect of increasing the content of ketone carbonyl units is also seen in the spectra in Figure 2b. The high-field portion of the cluster of ketone carbonyl resonances, observed in the 205−209 ppm region, has greater intensity in the spectrum of sample C, due to its higher content of C═O groups, compared to the spectra of samples A and B. Relative increases in the intensities of the peaks in the high-field portion of the

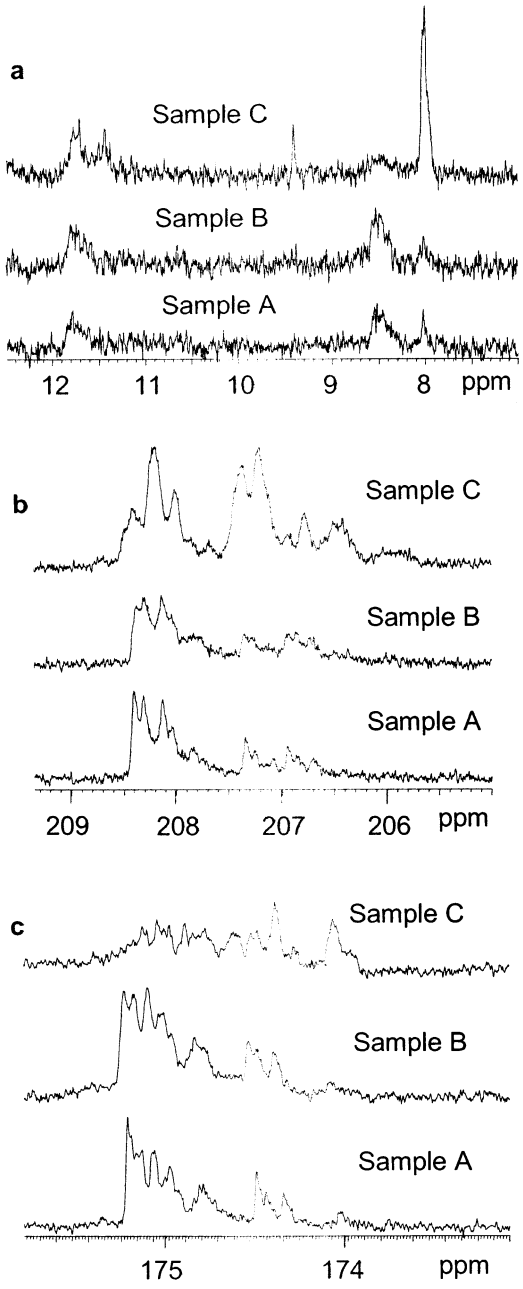

Figure 2. Expansions from the 188 MHz ^{13}C NMR spectra of terpolymer samples A, B, and C: (a) methyl and aliphatic chain end resonance region, (b) ketone carbonyl resonance region, and (c) ester carbonyl resonance region.

cluster of ester carbonyl resonances (173−175 ppm) are also seen in the spectrum from sample C (Figure 2c). Because of its lower content of *n*-butyl acrylate and ethylene monomer units relative to ketone carbonyl units, sample C produces a spectrum with lower intensities for the resonances in the downfield portion of the peak cluster from the ester carbonyl carbons (attributed to triads such as EBE and EBB) compared to the corresponding resonances in the spectra of samples A and B. The pattern for both types of ester carbonyl resonances are highly complex; the large number of peaks indicates that the chemical shifts are sensitive to pentad or heptad sequences. Tacticity effects should also be considered, since triads with two adjacent *n*-butyl acrylate units can exist in *meso* or *racemic* configurations. Since the number of triads containing

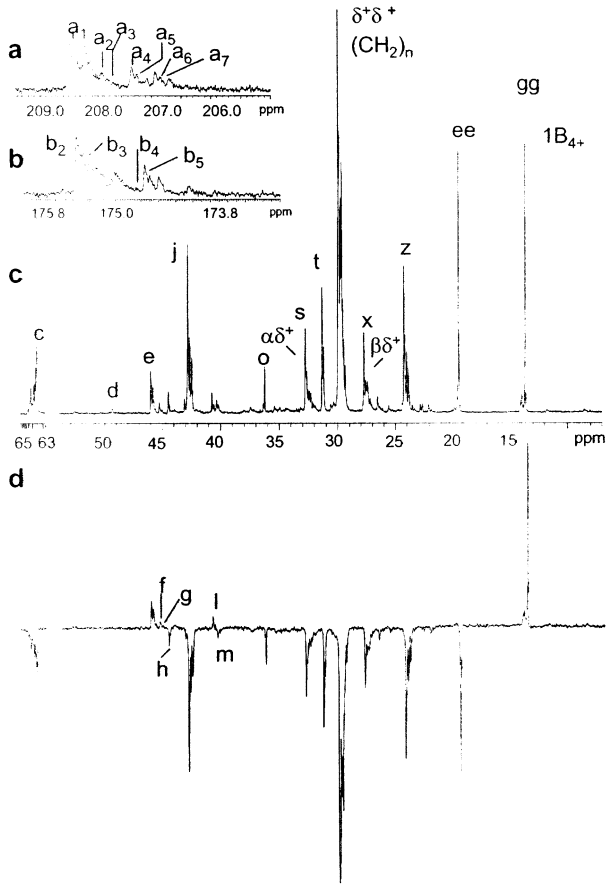

Figure 3. Selected regions from the 188 MHz ^{13}C NMR spectrum of sample A: (a) ketone carbonyl resonance region, (b) ester carbonyl resonance region, (c) butoxy and aliphatic resonance region, and (d) DEPT spectrum; $\theta = 135°$.

two B units is quite small, these effects would be minor. However, the high-field portions of these regions are derived from C═O-containing triads.

General assignments of peak clusters can be determined from the 1D ^{13}C NMR data, but specific peak assignments were provided by experiments such as DEPT, in addition to 2D PFG-HMQC and HMBC experiments that afforded better spectral dispersion and atomic connectivity information. DEPT experiments yielded multiplicity assignments for the various resonances. Figure 3d shows the DEPT-135[16] spectrum for sample A. The positive resonances for methyl (gg) and methine carbons (g and l) are readily distinguished from the negative resonances of methylene carbons. This was useful for distinguishing ^{13}C resonances of methines from those of methylenes. Closely spaced resonances such as those near 45.3 and 44.7 ppm could be attributed to CH carbons of BEC triads (g) and CH_2 carbons (h) of ECBE tetrads, respectively. The resonance due to the methine carbon of ECBE tetrads (l, $\delta = 40.79$) could also be distnguished from the resonance of methylene carbon (m, $\delta = 40.43$) of BEC triads. Results from the DEPT experiments are summarized in the sixth column of Table 3.

PFG-HMQC and HMBC 2D NMR Spectra. Figure 4 shows the PFG-HMQC 2D NMR spectra of samples A and C labeled with cross-peak assignments for structures **2**, **3**, **4**, and **7**. Both spectra exhibit the most prominent correlations between the ^{1}H and ^{13}C resonances of directly bound atoms in methine, methylene, and methyl groups. At $\delta_H = 1.31$, a very intense cross-

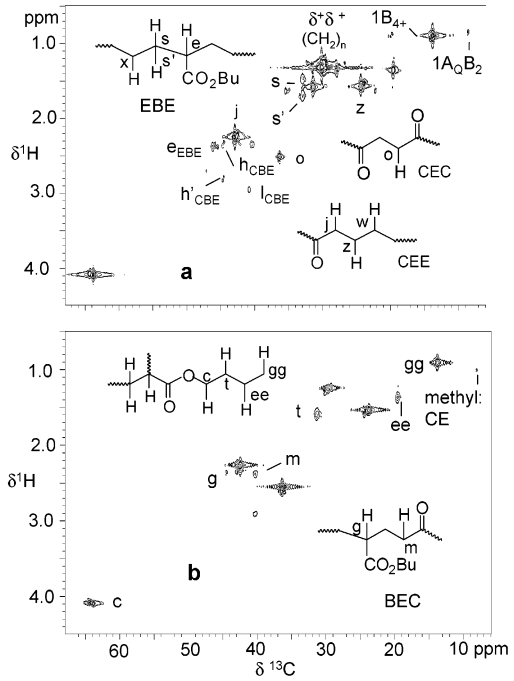

Figure 4. Selected regions from the PFG-HMQC 2D-NMR spectra of samples A (a) and C (b).

peak is observed at $\delta_C = 30.08$, which is attributed to $\delta^+\delta^+$ methylene carbons in long ethylene sequences. Cross-peaks for the methylenes in the butyl ester groups (Figure 4b, cross-peaks c, t, and ee) and for the methyl group (cross-peak gg) as well as the CH_2's of CEE triads (cross-peak j from $\alpha^C\delta^+$ and cross-peak z from $\beta^C\delta^+$ carbons) and the equivalent methylenes of CEC triads (cross-peak o) are readily apparent in both spectra. Nonequivalent ^{1}H resonances (1.68 and 1.46 ppm, s and s′ in Figure 4a) correlated with the peak at $\delta_C = 32.84$ are assigned to α^B methylene carbons in EBE triads. When the HMQC spectra of samples C and A are compared, cross-peaks attributed to the methylenes and the terminal methyls of the butyl ester groups as well as the methylenes from CEE, CEC and BEC triads predominate in the spectrum of sample C (Figure 4b). Cross-peaks from α^B methylene groups of EBE triads are extremely weak. In the HMQC spectrum from sample C, a cross-peak attributed to the terminal methyl in CE structures found in chain ends and branches terminating in ethyl ketone units is also observed at $\delta_C = 8.02$ and $\delta_H = 1.02$.

Peaks in the HMQC spectrum were assigned with the aid of HMBC results. Figure 5 shows the PFG-HMBC spectrum from sample A. This spectrum exhibits correlations between the resonances of ^{1}H and ^{13}C atoms separated by two and three bonds. Along each ^{1}H chemical shift, the cross-peaks in the HMBC spectra are labeled with a lower case letter corresponding to the letter used to label one-bond C−H correlations in the HMQC spectrum, and a numerical subscript is used to uniquely identify each HMBC correlation at that ^{1}H chemical shift. This accommodates the fact that a single proton resonance will exhibit correlations to several carbon resonances in the HMBC spectrum. Multiple-bond C−H correlations for CEE triads are seen along $\delta_H = 2.25$, the shift of the $\alpha^C\delta^+$ methylene protons (cross-peaks j_1, j_2, and j_3), and along $\delta_H = 1.56$, the shift of $\beta^C\delta^+$ methylene protons (cross-peaks z_1, z_2, and z_3). The multiple-bond correlation between the resonances

Table 3. Chemical Shift Assignments Poly(*n*-butyl acrylate-*co*-carbon monoxide-*co*-ethylene)[28]

		assignments			DEPT	chemical shift assignments				integral range		^{13}C: integral value[b]		
						polymer A		polymer C						
region	peak	carbon type	structure	monomer sequence[c]	result[a] s/d/t/q	δ^{13}C[d]	δ^{1}H	δ^{13}C	δ^{1}H	start	end	*A*	*B*	*C*
a	a_1		CO	EECEE	n.d.	208.39	n.d.			209.03		30	26	44
	a_2		CO	BECEX	n.d.	207.84	n.d.				207.78			
	a_3		CO	XCE**C**ECX	n.d.			207.70	n.d.	207.78				
	a_4		CO	XEECECE	n.d.	207.41	n.d.							
	a_5		CO	XCE**C**ECX	n.d.			207.37	n.d.					
	a_6		CO	EECBE	n.d.	206.91	n.d.		n.d.					
	a_7		CO	XCE**C**ECX	n.d.			206.78	n.d.		205.57	15	17	66
b	b_1		CO	A_QB_2	n.d.	176.49	n.d			176.45	176.05	1.5	2.8	1.1
	b_2		CO	EBE	n.d.	175.43	n.d			176.05				
	b_3		CO	EBB	n.d.	175.23	n.d.				174.70	29	41	19
	b_4		CO	ECBEX	n.d.	174.67	n.d			174.70	174.63	0.7	1.3	2.0
	b_5		CO	XEBEC	n.d.	174.46	n.d.			174.63	173.90	5.8	10.0	17.6
c	c_1	$^{e}E_4$	CH_2	EBE	t	64.30	4.07			64.82				
	c_2	E_4	CH_2	A_QB_2	t	64.12	4.10							
	c_3	E_4	CH_2	EBE	t	63.79	4.09				63.46	42	56	38
d		C_{AQB2}	C	A_QB_2	s	49.34	n.d.			53.16	48.63	6.5	4.8	5.8
e	e_1	CH_{EBE}	CH	EBE	d	46.16	2.38			46.71				
	e_2	CH_{EBE}	CH	EBE	d	45.82	2.35				45.47	21.2	24.0	11.7
f		CH_{EBB}	CH	EBB	d	45.46	2.39			45.47				
g		CH_{XEBEC}	CH	XEBEC	d	45.31	2.39				44.85	4.5	5.3	7.6
h		$\alpha^C\alpha^B$	CH_2	ECBE	t	44.70	2.83			44.85				
		$\alpha^C\alpha^B$	CH_2	ECBE	t	44.70	2.36							
I		$\alpha^C\,\alpha^B$	CH_2	CBB	t	44.53	2.77							
		$\alpha^C\alpha^B$	CH_2	CBB	t	44.53	2.32				44.18	7.4	8.4	15.4
j		$\alpha^C\,\delta^+$	CH_2	CEE	t	42.91	2.25			43.42	42.25	78	68	143
k		α^C	CH_2	ECE-c.e.[f]	t			42.24	2.26	42.25	41.48	4.4	3.7	4.5
l		CH_{ECBEX}	CH	ECBEX	d	40.79	2.94			41.02				
m		$\alpha^C\,\beta^B$	CH_2	BEC	t	40.43	2.34							
n		CH_{CBB}	CH	CBB	d	40.30	2.92				39.76	15.3	17.4	27.0
o		$\alpha^C\,\beta^C$	CH_2	CEC	t	36.35	2.52			36.81				
p		$\alpha^C\,\alpha^{CH3}$	CH_2	CE-c.e.	t			35.74	2.28		35.64	12.4	9.1	67
q		αA_QB_2	CH_2	A_QB_2	t	33.80	1.64			34.64	33.58	8.6	4.7	0.7
r		$\alpha^B\,\beta^+$	CH_2	ECBE	t	32.50	1.66			33.58				
		$\alpha^B\beta^+$	CH_2	ECBE	t	32.50	1.50							
s	s_1	$\alpha^B\,\gamma^+$	CH_2	EBEEX	t	32.84	1.68							
		$\alpha^B\gamma^+$	CH_2	EBEEX	t	32.84	1.46							
	s_2	$\alpha^B\gamma^+$	CH_2	XEBEC	t	32.54	1.69							
		$\alpha^B\gamma^+$	CH_2	XEBEC	t	32.54	1.46				31.58	61	67	41
t		E_3	CH_2	EBE	t	31.40	1.58			31.58	30.84	44	55	40
u		$\delta^+\delta^+$	CH_2	XEEEX	t	30.08	1.31			30.84				
v		$\gamma^B\gamma^+$	CH_2	XEEBE	t	30.05	1.30							
w		$\gamma^C\delta^+$	CH_2	CEEXX	t	29.74	1.27				28.77	323	264	152
x		$\beta^B\gamma^+$	CH_2	EBE	t	27.89	1.36			28.07	26.84	56	63	30.4
y		$\beta^C\alpha^B$	CH_2	BEC	t	26.50	1.84			26.83	25.90	12.1	14.0	15.5
z		$\beta^C\delta^+$	CH_2	CEE	t	24.31	1.56			24.58				
aa		$\beta^C\delta^+$	CH_2	ECE-c.e.	t			24.04	1.55		23.42	79	72	133
bb		$2A_QB_4$	CH_2	A_QB_4	t	23.38	1.25			23.42				
cc		$2B_4$	CH_2	B_4[g]	t	23.06	1.31				23.00	2.6	2.2	0.3
dd		$\beta^C\beta^B$	CH_2	CEB	t	22.22	1.64			22.33	21.60	4.9	6.0	6.5
ee		E_2	CH_2	EBE	t	19.57	1.35			20.24	18.79	45	57	37
ff		$1A_QB_4$	CH_3	A_QB_4	q	14.04	0.93			14.53				
gg		E_1	CH_3	EBE	q	13.75	0.89				13.10	49	62	45
hh		α^BE	CH_3	BE-c.e.	q	11.17	0.89			11.4				
ii		$1B_2$	CH_3	B_2[h]	q	10.72	0.88				10.58	1.5	1.8	1.1
jj		$1A_QB_2$	CH_3	A_QB_2	q	8.51	0.84			8.67				
kk		β^C	CH_3	CE-c.e.	q			8.02	1.02		7.45	3.4	2.9	6.0

[a] DEPT experiment results s, d, t, and q are quaternary, methine, methylene, and methyl carbon resonances, or n.d. means not determined. [b] Relative error better than 10%. [c] Because carbon monoxide (C) contributes only carbons to the backbone, the chemical shifts of the atoms in the central unit are sensitive to the structures on the other side of the C units. In n-add resonance assignments, fictitious units are sometimes used in this table that are designated by the symbol X. [d] Relative to internal hexamethylsiloxane (HDMS), estimated error 0.005 ppm based; digital resolution is 0.08 Hz/point (0.0004 ppm/point) and the average line width of 1 Hz. [e] E_4, E_3, and E_2 are methylenes, and E_1 is terminal CH_3 in the ester. [f] Lower case designate units in chain ends and branches. [g] Designates a butyl branch due to SCB-forming reactions and is equivalent to a four-carbon branch formed by incorporation of 1-hexene. [h] Designates an ethyl branch due to SCB-forming reactions and is equivalent to a two-carbon branch formed by incorporation of 1-butene.

of $\alpha^C\beta^C$ methylene protons and ketone carbonyl carbons of CEC triads is seen at $\delta_H = 2.52$ (cross-peak o_1). A correlation to the $\alpha^C\beta^C$ methylene proton resonance is also seen when a ^{13}C atom exists on the adjoining $\alpha^C\beta^C$ methylene carbon (cross-peak o_2).

Cross-peaks for the butyl units of ester groups are also seen in Figure 5. Multiple-bond C−H correlations from the methyl group of the butyl ester are observed between the proton resonances at $\delta_H = 0.89$ and the resonances of neighboring methylene carbons (cross-peaks gg_1 and gg_2). The proton resonances from the butoxy methylene groups exhibit correlations along $\delta_H = 4.09$ to the resonances of adjacent methylene carbons (cross-peaks c_2 and c_3) and to the ester carbonyl

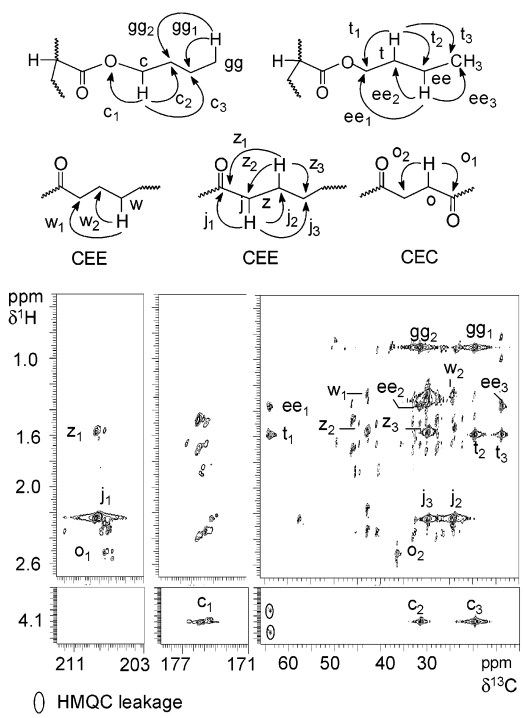

Figure 5. Selected regions from the PFG-HMBC 2D-NMR spectra of sample A with ester, CEE, and CEC cross-peak assignments.

carbon (cross-peak c_1). The proton resonances of the methylene group directly bonded to the terminal methyl are observed at $\delta_H = 1.35$. This resonance is correlated with the carbon resonances of adjacent methylene carbons (cross-peaks $ee_1$and ee_2) and the methyl carbon (cross-peak ee_3). Multiple-bond C−H correlations are also seen along $\delta_H = 1.58$ correlating the methylene proton resonances and the resonances of adjacent methylene carbons (cross-peak t_1 and t_2) and to the methyl carbon (cross-peak t_3). Since the butyl ester groups of this sample are present in various triad (and higher) sequences, complex C−H correlation patterns are evident in the HMBC spectrum.

Figure 6 shows expansions of selected regions from the PFG-HMBC spectrum of sample A, containing cross-peaks from multiple bond correlations in EBE triads. The $\alpha^B\delta^+$ methylene has nonequivalent protons with ^{1}H chemical shifts of 1.46 (s) and 1.68 (s′). These ^{1}H resonances are both correlated to the resonances of the ester carbonyl carbon (cross-peaks s_1 and s_1'), the methine carbon (CH_{EBE}, cross-peaks s_2 and s_2'), the β-methylene carbon ($\beta^B\gamma^+$, cross-peaks s_4 and s_4'), and the γ-methylene carbon ($\gamma^B\gamma^+$, cross-peaks s_3 and s_3'). Two cross-peaks (s_5 and s_5') occur at the ^{1}H chemical shifts of the nonequivalent protons of $\alpha^B\gamma^+$ methylenes; these $\alpha^B\gamma^+$ nonequivalent protons also show correlations with the resonance at $\delta_C = 32.80$, which is attributed to the $\alpha^B\beta^+$ methylene carbon that is also bonded to CH_{EBE}. The resonance from the methine proton (CH_{EBE}) at the ^{1}H chemical shift of 2.38 is correlated with the ^{13}C resonances of the ester carbonyl (cross-peak e_1), the α^B methylene (cross-peak e_2), and the β-methylene (cross-peak e_3). The ^{1}H resonances of the β-methylene along $\delta = 1.36$ are correlated with the ^{13}C resonances of the methine (CH_{EBE}, cross-peak x_1) and to adjacent methylenes ($\alpha^B\gamma^+$, cross-peak x_2 and $\gamma^B\gamma^+$, cross-peak x_3).

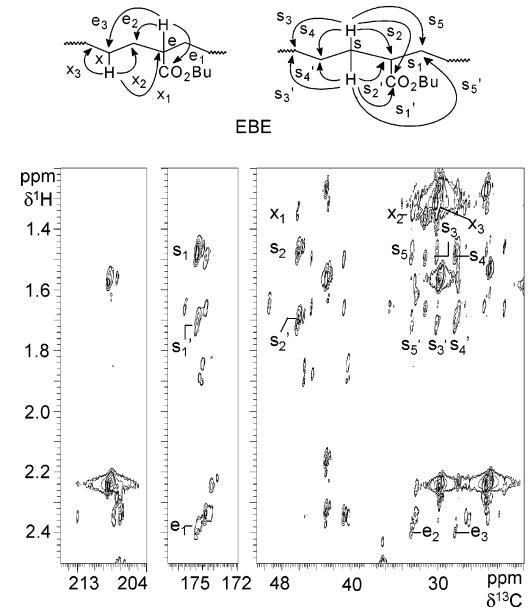

Figure 6. Selected regions from the PFG-HMBC 2D-NMR spectra of sample A with cross-peak assignments of EBE triads.

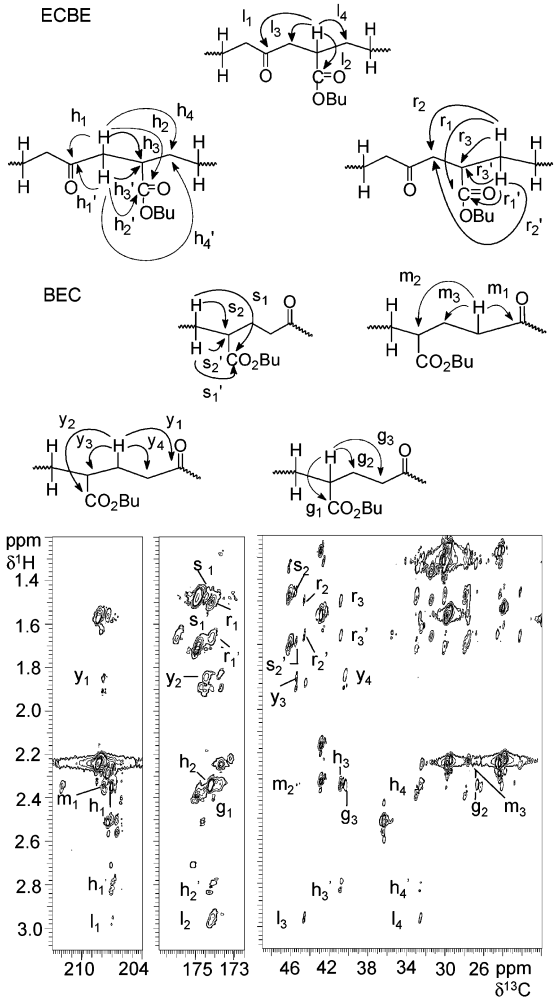

Figure 7. Selected regions from the PFG-HMBC 2D-NMR spectra of sample A with cross-peak assignments of ECBE tetrads and BEC triads.

Figure 7 shows cross-peak assignments of ECBE tetrads in the PFG-HMBC spectrum of sample A. Resonances from nonequivalent protons of $\alpha^C\alpha^B$ meth-

ylene groups at the ^{1}H chemical shifts of 2.36 and 2.83 are correlated to carbon resonances of the ketone carbonyl (cross-peaks, h_1, h_1'), ester carbonyl (cross-peaks h_2, h_2'), methine carbon (CH_{ECBE}, cross-peaks h_3, h_3'), and methylene ($\alpha^B\beta^+$, cross-peaks h_4, h_4'). The proton resonance at the ^{1}H chemical shift of 2.94 for CH_{ECBE} is correlated to ^{13}C resonances of the ketone carbonyl (cross-peak l_1), ester carbonyl, (cross-peak l_2), methylene, ($\alpha^C\alpha^B$, cross-peak l_3), and methylene, ($\alpha^B\beta^+$, cross-peak l_4). The resonances for the nonequivalent protons of the $\alpha^B\beta^+$ methylene group at the ^{1}H chemical shifts of 1.50 and 1.66 ppm are correlated with the ^{13}C resonances of the ester carbonyl (cross-peaks r_1 and r_1'), the methine (CH_{ECBE}, cross-peaks r_3 and r_3'), and the methylene ($\alpha^C\alpha^B$, cross-peaks r_2 and r_2').

The cross-peak assignments of BEC triads are also shown on the structures at the top of Figure 7. Resonances from nonequivalent protons of α^B methylene groups at ^{1}H chemical shifts of 1.69 and 1.46 are correlated to the ^{13}C resonances of the ester carbonyl (cross-peaks s_1, s_1') and methine carbon (CH_{BEC}, cross-peaks s_2, s_2'). The CH_{BEC} proton resonance at $\delta_H = 2.39$ is correlated to the ^{13}C resonances of the ester carbonyl (cross-peak g_1), $\alpha^B\beta^C$ methylene carbon (cross-peak g_2), and $\alpha^C\beta^B$ methylene carbon (cross-peak g_3). The resonances from the protons of $\alpha^C\beta^B$ methylene groups along $\delta_H = 2.34$ are correlated with ^{13}C resonances of the ketone carbonyl (cross-peak m_1), $\alpha^B\beta^C$ methylene (cross-peak m_3), and CH_{BEC} methine (cross-peak m_2). The resonances from the protons of $\alpha^B\beta^C$ methylene groups at the chemical shift of 1.84 ppm are correlated with the ^{13}C resonances of the ketone carbonyl (cross-peak y_1), the ester carbonyl (cross-peak y_2), methine (CH_{BEC}, cross-peak y_3), and methylene ($\alpha^B\beta^C$, cross-peak y_4).

Other structures can also contain a ketone carbonyl group. Previous work by Bovey et al.[9,10] demonstrated that backbiting reactions in the polymerization of ethylene and carbon monoxide yielded ethyl ketone (**11**, Scheme 2) and butyl ketone (**12**, Scheme 2) branches. Bovey[9] assigned the methine carbon resonance of the ethyl ketone branch to the peak at $\delta = 52.6$, which does not agree with the assignment of Wu et al.,[26] who predicted the peak would occur at 31.4 ppm on the basis of the Lindeman and Adams formula[27] and Wu's ketone parameters. The higher field resonance is explained by the effect of the methylene that is between the methine and the carbonyl units. Wu and co-workers assigned the weak ^{13}C peaks in the 50−52 ppm region to methine carbon atoms in branches next to carbonyl units. Bovey assigned the resonance of the methine carbon of the butyl ketone branch at $\delta = 51.6$, which is similar to that predicted by Wu and co-workers at $\delta = 49.8$. (Wu's structure is terminated by a methyl group while Bovey's has a continuous chain.) Weak resonances observed in the 50−53 ppm region of the ^{13}C NMR spectrum of sample A (Figure 3c) and the DEPT spectrum (Figure 3d) confirm these can arise from methine carbons.

Resonances consistent with ketone-containing chain ends are also observed; these are more apparent in the spectra of sample C which has a higher ketone carbonyl content than sample A. Figure 8 shows C−H correlations in the PFG-HMBC spectrum of sample C corresponding to chain ends and branches terminating in ethyl ketone units. Along $\delta_H = 1.02$, the chemical shift for the terminal methyl protons, correlations are observed with the ^{13}C resonances of the ketone carbonyl (cross-peak kk_1) and the α^C-methylene of the ethyl

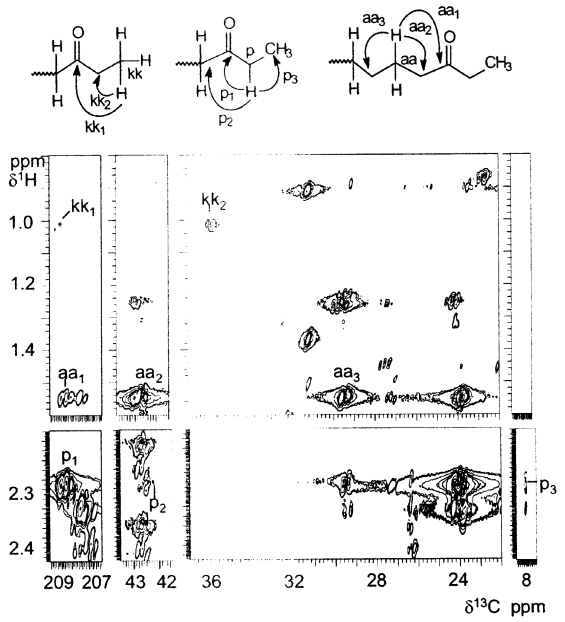

Figure 8. Selected regions from the PFG-HMBC 2D-NMR spectra of sample C with cross-peak assignments of CE diads.

ketones (cross-peak kk_2). The ^{1}H resonance at 2.28 ppm of the α^C-methylene protons of the ethyl ketones is correlated with ^{13}C resonances of the ketone carbonyl (cross-peak p_1), α^C -methylene (cross-peak p_2), and the terminal methyl (cross-peak p_3) carbons. Correlations are apparent for ethylene units adjoining the ethyl ketone carbonyl. Along $\delta_H = 1.55$, the chemical shift for the protons of the $\beta^C\gamma^+$ methylene, correlations are observed with the ^{13}C resonances of the ketone carbonyl (cross-peak aa_1), the $\alpha^C\gamma^+$ methylene (cross-peak aa_2), and the $\gamma^C\gamma^+$ methylene (cross-peak aa_3).

Evidence for short-chain-branch-forming reactions involving only ethylene units is especially noticeable in the spectra of sample A. Resonances for structures that result from backbiting reactions are observed in the ^{13}C NMR spectrum (Figure 3c). The $1B_2$ ethyl peak is seen at $\delta_C = 10.72$, and the $2B_4$ butyl peak is detected at 23.06 ppm. NMR results also indicate SCB-forming reactions involving *n*-butyl acrylate units. Two peaks at $\delta_C = 27.58$ and 23.38 are tentatively assigned to $2A_QB_2$ and $2A_QB_4$ structures, respectively. In the ^{13}C NMR spectrum (Figure 3c), peak d at $\delta_C = 49.34$ is attributed to the quaternary carbon in the A_QB_2 structure. Since there are no protons attached to the quaternary carbon, this peak was not observed in the DEPT spectrum (Figure 3d), and C−H correlations at $\delta_C = 49.34$ were not detected in the PFG-HMQC spectrum. However, in the PFG-HMBC spectrum as shown in Figure 9, a correlation is observed between the resonances of the methyl protons of the ethyl branch ($\delta_H = 0.84$) and the ^{13}C resonance of the quaternary carbon (cross-peak jj_1) and with the ^{13}C resonances for a $2A_QB_2$ carbon (cross-peak jj_2). The proton resonance at $\delta_H = 1.64$ is attributed to the main-chain methylenes α to a A_QB_2 branch since it is correlated with the ^{13}C resonance of the quaternary carbon (cross-peak q_2) and to ester carbonyl of the opposing branch (cross-peak q_1). At the proton chemical shift of 4.10 ppm (assigned to the methylenes of the ester), a correlation is seen with the ^{13}C resonance of the ester carbonyl region (cross-peak c_1). Figure 9 also shows evidence with A_QB_4 structures. A correlation is seen at $\delta_H = 0.93$, the resonance of the methyl proton and the carbon resonance of methylenes

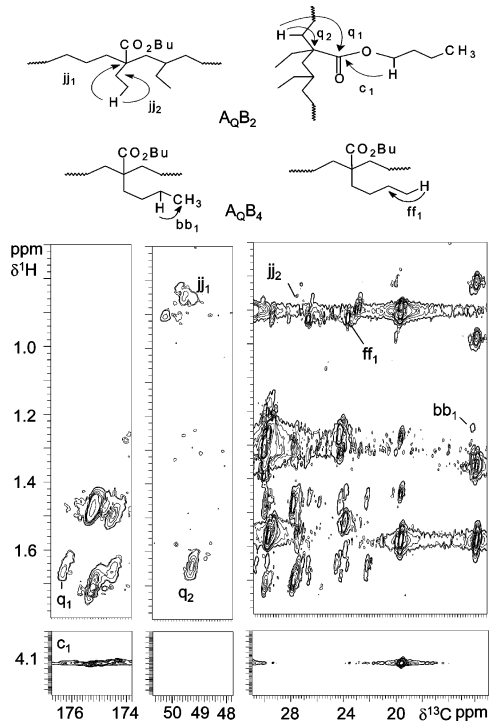

Figure 9. Selected regions from the PFG-HMBC 2D-NMR spectra of sample A with cross-peak assignments of A_QB_2 structures.

(cross-peak ff_1), which might be attributed to coupling between $1A_QB_4$ methyl proton and a $2A_QB_4$ carbon. There is also a correlation between the proton resonance, possibly from $2A_QB_4$, at 1.25 ppm and the carbon resonance of $1A_QB_4$ (cross-peak bb_1). Unequivocal proof for the existence of these structures requires dramatic improvements in both sensitivity and spectral dispersion as would be obtained from ^{13}C labeling.

Quantitative NMR Analysis. For the quantitative analysis of a terpolymer sample, three separate spectra were collected with gated decoupling and a 30 s relaxation delay. NMR experiments on sample A indicated that this delay ($3 \times T_1$ for the carbonyl carbons which have the longest relaxation times) would ensure suppression of the nuclear Overhauser effect (NOE) and achieve reasonable relaxation. The integrated areas are presented in the form of carbons per 1000 carbons of polymer. The integrals for resolved resonances in the quantitative spectra of samples A, B, and C are shown in the last three columns of Table 3.

Resonances from 209.03 to 205.57 ppm are observed for the ketone carbonyl carbons which includes n-ad structures derived from ECE triads (i.e., EECEE and EECEC, etc.) and ECB triads (i.e., EECBE and ECBEE, etc.) as well as carbonyl-containing chain ends and branches. The integrated areas for this region of the spectrum were measured to be 45 for sample A, 43 for sample B, and 110 for sample C with its higher ketone carbonyl content. Overlapping peaks in the 209.03−207.78 ppm region are assigned to carbonyl carbons of EECEE pentads. Resonances in the 207.78−205.57 ppm region are attributed to CE**C**EC and EE**C**EC pentad structures. In addition, the resonance for the ketone carbonyl carbon in EE**C**BE pentads (δ = 206.91) is found in this region.

Resonances for the ester carbonyl carbons are observed in the 176.45−173.90 ppm region. The integrated areas for this region were measured as 37 for sample A, 55 for sample B, and 40 for sample C. The resonance for the ester carbonyl carbon in the ECBE tetrad is assigned to δ = 174.67.

Resonances for methylenes in n-ads derived from EECEE pentads are observed from 43.42 to 41.48 ppm for $\alpha^C\delta^+$ and from 24.58 to 23.42 ppm for $\beta^C\delta^+$. As expected, for the spectrum of sample A, the integrated areas (82) for α-methylenes are approximately equal to that of the β-methylenes (79). This trend is also seen in the integration values in the spectrum of sample B ($\alpha^C\delta^+$, 72; $\beta^C\delta^+$, 72). However, for the spectrum of sample C, the value of the integrated area of α^C methylenes is 148, which is higher than that of β^C methylenes (133); this is possibly due to a contribution to the integral from overlapping resonances of α^C methylenes in chain ends and branching structures that are in greater abundance. For each of the samples, areas of $\alpha^C\delta^+$ or $\beta^C\delta^+$ are approximately 3 times the integral for the ketone carbonyl resonances of these pentads, consistent with partial saturation of the ketone carbonyl resonances which have longer T_1's than the proton-bearing $\alpha^C\delta^+$ and $\beta^C\delta^+$ methylene carbons.

Resonances of methylenes in ECECE pentad sequences are observed in the 36.81−35.64 ppm region. The values of the integrated areas were 12.4, 9.1, and 67 for the spectra of samples A, B, and C, respectively. The ratio of the integrated values of EECEE to ECECE structures in samples A, B, and C were approximately 7:1, 8:1, and 2:1, respectively. As ketone carbonyl content in the sample increased, a much larger number of ECECE structures were observed.

The integrated areas for sequences that contain a butyl group can be analyzed by considering the resonances (64.82−63.46 ppm) for the methylene carbon α to the oxygen of the ester group. For the spectrum of sample A, the integral equals 42, which is higher than that of the ester carbonyl carbon (37); however, the latter values are attenuated by the longer relaxation time for the ester carbonyl carbons. For the butyl ester group, the integral for the methylene carbon α to oxygen is comparable to those for the methylene carbon β to oxygen (44, 31.58−30.84 ppm) and to the methylene carbon γ to oxygen (45, 20.24−18.79 ppm). As expected, the integral (49) of the carbon of the terminal methyl (14.53−13.10 ppm) is higher than the neighboring ester methylenes, since resonances in this region can also be assigned to terminal methyls on branches (due to backbiting reactions) that contain four or more carbons ($1B_{4+}$). In comparison to the integrals of methylenes of the ester group, much higher values are observed for the integrated area (61) attributed to methylene carbons that are α to the methine of the butyl acrylate ($\alpha^B\gamma^+$, 33.58−31.58 ppm) as well as that of the integrated region (56) calculated for methylene carbons that are β to the methine of the butyl acrylate ($\beta^B\gamma^+$, 28.07−26.84 ppm). The higher values are due to overlapping resonances of methylene carbons that are α and β to methines of branches in polyethylene segments.

Physical Properties. Examination of the number- and weight-average molecular weights as well as the polydispersity index (PDI: M_w/M_n) in Table 1 shows that each of the terpolymer samples contains a high molecular weight component. All of the samples are highly branched as evident from the g' values (where g' is the ratio of intrinsic viscosities of branched to linear polymers across the distribution). The NMR data show that short chain branches from backbiting reactions that

involve ethylene as well as *n*-butyl acrylate units affect the physical properties. Spectral results also indicate that carbonyl-containing branches and chain ends are more prominent in sample C, with its higher ketone carbonyl content. The physical analysis shows that sample C with the lowest g' value is the most highly branched. This degree of branching in sample C lowers the melt viscosity as shown by its relatively high melt index value M_I as compared to samples A and B.

Conclusions

The data presented here indicate the potential of high-field PFG 2D HMQC and HMBC experiments in proving the existence of specific structures in complex terpolymer samples. These NMR studies are especially valuable for providing unambiguous structural assignments when traditional methods involving 1D-NMR and systematic variation of monomer feed ratios are not sufficient. The resonance assignments that follow from this analysis will be useful for planned studies to model reaction kinetics and to investigate structure−property relationships. This research tackled the difficult problem of determining the structures present in a complex mixture of this terpolymer. The general methodology illustrated by these high-temperature PFG experiments will be useful for the analyses of other complex copolymers and terpolymers. Work is continuing on the development and use of isotopic labeling and 3D-NMR techniques to obtain additional simplification, dispersion, and selective enhancement of the resonances in the complex spectra from these polymers. These new NMR methods will provide more resonance assignments and proof of the existence of many additional key structures.

Acknowledgment. The authors acknowledge the National Science Foundation (DMR-0073346 and DMR-0324964) and E.I. du Pont de Nemours and Co for support of this research and the Kresge Foundation and donors to the Kresge Challenge program at the University of Akron for funds used to purchase the 750 MHz NMR instrument used for this work. Thanks are due to V. Dudipala, J. Massey, and S. Stakleff for their support in maintaining the NMR facilities used in this work.

References and Notes

(1) Liu, W.; Ray, D. G., III.; Rinaldi, P. L.; Zens, T. *J. Magn. Reson.* **1999**, *140*, 482.
(2) Liu, W.; Rinaldi, P. L.; McIntosh, L. H.; Quirk, R. P. *Polym. Prepr. (Am. Chem. Soc., Div. Polym. Chem.)* **2000**, *41*, 30.
(3) Liu, W.; Ray, D. G., III.; Rinaldi, P. L. *Macromolecules* **1999**, *32*, 3817.
(4) Liu, W.; Rinaldi, P. L.; McIntosh, L. R.; Quirk, R. P. *Macromolecules* **2001**, *34*, 4757.
(5) Sahoo, S. K.; Zhang, T.; Reddy, V.; Rinaldi, P. L.; McIntosh, L. H.; Quirk, R. P. *Macromolecules* **2003**, *36*, 4017.
(6) Muller, L. *J. Am. Chem. Soc.* **1979**, *101*, 4481.
(7) Bax, A.; Griffey, R. H.; Hawkins, B. L. *J. Am. Chem. Soc.* **1983**, *105*, 7188.
(8) Bax, A.; Summers, M. F. *J. Am. Chem. Soc.* **1986**, *108*, 2093.
(9) Bovey, F. A.; Gooden, R.; Schilling, F. C.; Winslow, F. H. *Macromolecules* **1988**, *21*, 938.
(10) Bovey, F. A.; Gooden, R.; Schilling, F. C. *Polym. Prepr. (Am. Chem. Soc., Div. Polym. Chem.)* **1987**, *28*, 238.
(11) Bruch, M. D.; Payne, W. G. *Macromolecules* **1986**, *19*, 2712.
(12) McGrath, J. E.; Robeson, L. M.; Nowlin, T. E.; Joesten, B. L.; Wise, E. W. In *Applications of Polymer Spectroscopy*; Brame, E. G., Ed.; Academic: New York, 1978; pp 41−55.
(13) McCord, E. F.; Shaw, W. H., Jr.; Hutchinson, R. A. *Macromolecules* **1997**, *30*, 246.
(14) Zimm, B. H.: Stockmayer, W. H. *J. Chem. Phys.* **1949**, *17*, 1301.
(15) *Annual Book of ASTM Standards*; American Society for Testing and Materials: West Conshohocken, PA, 2001; Vol. 08.01, p 260.
(16) Dodrell, D. M.; Pegg, D. T.; Bendell, M. R. *J. Magn. Reson.* **1982**, *48*, 323.
(17) Shake, A. J.; Barker, P. B.; Freeman, R. *J. Magn. Reson.* **1985**, *64*, 547.
(18) Carman, C. J.; Wilkes, C. E. *Rubber Chem. Technol.* **1971**, *44*, 781.
(19) Dorman, D. E.; Otocka, E. P.; Bovey, F. A. *Macromolecules* **1972**, *5*, 574.
(20) Randall, J. C. *J. Macromol. Sci., Rev. Macromol. Chem. Phys.* **1989**, *C29*, 201.
(21) The proposed system of nomenclature is necessary to distinguish structures associated with resonances that are better resolved using high-field NMR instruments. Labeling the backbone carbon permits assignment of unique identifiers, especially for nonequivalent structures (e.g., BEC and CEB), which can then be correlated to their distinctive NMR resonances.
(22) In this case, the term "branch" is used loosely, and the branch unit is formed by the replacement of the backbone methylene C−H bonds with a C═O bond.
(23) *Encyclopedia of Polymer Science and Technology*, 2nd ed.; John Wiley and Sons: New York, 1989; Vol. 6, pp 383−429.
(24) Randall, J. C.; Ruff, C. J.; Kelchtermans, M. *Pays-Bas* **1991**, *110*, 543.
(25) Randall, J. C.; Ruff, C. J.; Kelchtermans, M.; Gregory, B. H. *Macromolecules* **1992**, *25*, 2624.
(26) Wu, T. K.; Ovenall, D. W.; Hoehn, H. H. In *Applications of Polymer Spectroscopy*; Brame, E. G., Ed.; Academic: New York, 1978; pp 19−40.
(27) Lindeman, L. P.; Adams, J. Q. *Anal. Chem.* **1971**, *43*, 1245.
(28) All assignments are based on the 2D-NMR data of polyBCE collected in this research. Comparisons to literature chemical shifts of model polymers are described in the text to support these assignments. Prior results were generally obtained in different solvents under different conditions so that chemical shifts do not necessarily agree.

MA035311J